KI REPORTS
KIReports.org
CLINICAL RESEARCH

Red Blood Cell AE1/Band 3 Transports in Dominant Distal Renal Tubular Acidosis Patients

Jean-Philippe Bertocchio[1,2,3,4], Sandrine Genetet[5,6], Lydie Da Costa[5,7,8], Stephen B. Walsh[9], Bertrand Knebelmann[10], Julie Galimand[8], Lucie Bessenay[11], Corinne Guitton[12], Renaud De Lafaille[13], Rosa Vargas-Poussou[3,14,15], Dominique Eladari[16,17,18] and Isabelle Mouro-Chanteloup[5,6,18]

[1]Renal and Metabolic Diseases Unit, Assistance Publique-Hôpitaux de Paris, European Georges Pompidou Hospital, Paris, France; [2]Faculty of Medicine, Paris Descartes University, Paris, France; [3]Reference Center for Maladies Rénales Héréditaires de l'Enfant et de l'Adulte (MARHEA), Paris, France; [4]Genito-urinary Medical Oncology and Research Department, MD Anderson Cancer Center, Houston, Texas, USA; [5]UMR_S1134, Integrated Red Globule Biology (IRGB), Inserm, University of Paris, Paris, France; [6]Team 1, Physiology of Normal and Pathologic Red Blood Cell, Institut National de la Transfusion Sanguine (INTS), Paris, France; [7]UMR_S1134, Inserm, Paris, France; [8]Service d'Hématologie Biologique, Assistance Publique-Hôpitaux de Paris, Hôpital Robert Debré, Paris, France; [9]Department of Renal Medicine, University College of London, London, UK; [10]Nephrology Department, Assistance Publique-Hôpitaux de Paris, Necker-Enfants Malades Hospital, Paris, France; [11]Pediatrics Department, University Hospital of Clermont-Ferrand, Clermont-Ferrand, France; [12]Pediatrics Department, Assistance Publique-Hôpitaux de Paris, Hôpital Bicêtre, Le Kremlin Bicêtre, France; [13]Nephrology Department, University Hospital of Bordeaux, Bordeaux, Aquitaine, France; [14]Institut National pour la Santé et la Recherche Médicale (INSERM), Unité Mixte de Recherche UMRS1138, Cordeliers Research Center, Paris, France; [15]Genetics Department, Assistance Publique-Hôpitaux de Paris, European Georges Pompidou Hospital, Paris, France; [16]Renal and Metabolic Diseases Department, CHU de la Réunion, Felix Guyon Hospital, Saint Denis, France; and [17]INSERM, UMRS 1283—European Genomic Institute for Diabetes, Lille, France

Introduction: Anion exchanger 1 (AE1) (*SLC4A1* gene product) is a membrane protein expressed in both kidney and red blood cells (RBCs): it exchanges extracellular bicarbonate (HCO_3^-) for intracellular chloride (Cl^-) and participates in acid—base homeostasis. AE1 mutations in kidney α-intercalated cells can lead to distal renal tubular acidosis (dRTA). In RBC, AE1 (known as band 3) is also implicated in membrane stability: deletions can cause South Asian ovalocytosis (SAO).

Methods: We retrospectively collected clinical and biological data from patients harboring dRTA due to a *SLC4A1* mutation and analyzed HCO_3^- and Cl^- transports (by stopped-flow spectrophotometry) and expression (by flow cytometry, fluorescence activated cell sorting, and Coomassie blue staining) in RBCs, as well as RBC membrane stability (ektacytometry).

Results: Fifteen patients were included. All experience nephrolithiasis and/or nephrocalcinosis, 2 had SAO and dRTA (dRTA SAO+), 13 dominant dRTA (dRTA SAO−). The latter did not exert specific RBC membrane anomalies. Both HCO_3^- and Cl^- transports were lower in patients with dRTA SAO+ than in those with dRTA SAO− or controls. Using 3 different extracellular probes, we report a decreased expression (by 52%, $P < 0.05$) in dRTA SAO+ patients by fluorescence activated cell sorting, whereas total amount of protein was not affected.

Conclusion: Band 3 transport function and expression in RBCs from dRTA SAO− patients is normal. However, in SAO RBCs, impaired conformation of AE1/band 3 corresponds to an impaired function. Thus, the driver of acid—base defect during dominant dRTA is probably an impaired membrane expression.

Kidney Int Rep (2020) **5,** 348–357; https://doi.org/10.1016/j.ekir.2019.12.020
KEYWORDS: acidosis, renal tubular; anion exchange protein 1; erythrocyte; hematologic diseases; nephrocalcinosis; nephrolithiasis

Correspondence: Jean-Philippe Bertocchio, Renal and metabolic diseases unit, European Georges Pompidou Hospital, 20 rue Leblanc, F-75908 Paris CEDEX, France. E-mail: jpbertocchio@gmail.com

[18]DE and IM-C contributed equally to this work.

Received 26 October 2019; revised 26 November 2019; accepted 31 December 2019; published online 13 January 2020

The anion exchanger type 1 (AE1 or band 3) is an integral membrane protein that exchanges intracellular bicarbonate (HCO_3^-) for extracellular chloride (Cl^-).[1] It is encoded by the *SLC4A1* gene that produces 2 isoforms: one expressed in the red blood cell (RBC), also known as band 3, and one expressed in α-intercalated cells (α-ICs) of the renal collecting duct (kAE1), which

lacks 65 N-terminal amino acids.[2] *SLC4A1* gene mutations have been reported to cause either RBC or renal abnormalities. In RBC membrane, band 3, which represents about 30% of the total amount of proteins, is part of a protein complex that plays an important role in the stability of RBC structure.[3,4] *SLC4A1* mutations affecting RBCs provoke abnormalities such as ovalocytosis or spherocytosis.[5] In the kidney, the main role of kAE1 is to extrude HCO_3^- at the basolateral membrane of α-ICs, which is a critical step for renal acidification. When impaired, intracellular HCO_3^- accumulates and blocks intracellular generation of protons and HCO_3^- from CO_2, and this ultimately inhibits apical proton secretion by the v-H^+-ATPase.[6] Accordingly, *SLC4A1* mutations affecting kAE1 lead to type 1 distal renal tubular acidosis (dRTA), characterized by abnormal proton secretion.[7,8] It is not known whether kAE1, like its RBCs' homolog band 3, plays a role as an anchoring structural protein. However, kAE1 has been described to be part of a protein macro-complex involving ankyrin.[9]

How *SLC4A1* mutations affect HCO_3^- transport in kidney is not completely understood. Based on heterologous expression studies in cell models or in *Xenopus* oocytes, some mutations have been proposed to provoke a mistargeting of the protein to the apical membrane, whereas others are thought to alter intrinsic transport properties of the protein, or to provoke an intracellular retention of the protein.[1,2] However, it is difficult to draw firm conclusions from these studies because the protein was not expressed in its natural environment. Furthermore, some experiments testing the effects of a mutation have yielded different results when the protein was expressed in different cell models. Indeed, a recent study in a mouse *knock-in* model with the p.R607H mutation, corresponding to p.R589H in humans, reported different results.[10] Interestingly, because kAE1 is a truncated isoform of RBCs' AE1, all mutations affecting kAE1 also affect band 3. Taking advantage of this, we tested in RBC the effects of *SLC4A1* mutations found in dRTA patients. We measured Cl^-/HCO_3^- transports and AE1/band 3 surface expression, as well as the RBC structural stability. Finally, we found that patients with dominant dRTA had both normal AE1 expression and function in RBCs, whereas those with recessive dRTA had both important morphological and functional anomalies.

METHODS

Population

All patients came from the European Georges Pompidou Hospital (Paris, France) and the Royal Free Hospital (London, UK). All (and parents if patients were <18 years old) gave informed consent. All experiments were performed in accordance with relevant guidelines and regulations, as well as the Declaration of Helsinki. All samples were collected in the INTS-CNRGS biobank, approved by the local ethics committee (CPP Ile-de-France II) and the French Research Ministry (ref. DC-2016-2872). Birth date, sex, clinical data at diagnosis, and biological data at diagnosis were retrospectively collected anonymously in accordance with the French regulatory board (ref. 2097359v0).

Red Blood Cell Indices, Reticulocyte Count, and Biochemistry Analyses

All ethylenediamine tetraacetic acid blood samples were immediately shipped at +4 °C. A blood smear was provided to avoid artifacts (echinocytes, acanthocytes, spiculated dense red cells). Routine RBC indices were centrally obtained for each sample using a Sysmex auto-analyzer (XN 5000, Sysmex, Kobe, Japan). Blood smear were carefully screened by 2 independent cytologists who validated RBC morphology anomalies after May−Grünwald Giemsa coloration (MGG).

Ektacytometry

A 100-μl quantity of blood from each patient was run on an ektacytometer (LoRRca MaxSis, RR Mechatronics, Hoorn, Netherlands).[5,11] Values for each patient were compared to those of an age-matched healthy control and to the reference values from the laboratory (R. Debré Hospital, Paris, France). Fresh blood was exposed to a shear stress and to an osmotic gradient. The laser beam diffraction pattern through the suspension was detected with a video camera. The RBC shapes changed from circular to elliptical as shear stress increased. Then, a deformability index or elongation index of cells was derived. The deformation of RBCs suspended in a viscous aqueous polyvinylpyrrolidone solution at defined values of applied shear stress of 30 Pa and at a constant temperature measurement of 37 °C was monitored as a continuous function of suspending medium osmolality. The ektacytometry curve pattern and remarkable points were recorded: (i) Omin, reflecting the surface area-to-volume ratio, that is, the osmolality at the minimal deformability in hypo-osmolar area, or the osmolality when 50% of the RBCs hemolyzed during the regular osmotic resistance test; (ii) EImax, corresponding to the maximal deformability index or elongation index; and (iii) the hyper point, or Ohyper, corresponding to the osmolality at half of the DImax or EImax, that is, the hydration state of the RBCs.

Cl^-/HCO_3^- Exchanger Activity Measurements

A 300-μl quantity of blood was washed 3 times in phosphate-buffered saline solution. Washed RBCs were resuspended in 25 ml hypotonic lysis buffer (7 mM KCl,

10 mM Hepes, pH 7.2 for HCO_3^- transport or 5 mM HPO_4, 1 mM ethylenediamine tetraacetic acid, pH 8.0 for Cl^- transport) for 40 minutes at +4 °C, followed by resealing for 1 hour at 37 °C in resealing buffer (100 mM KCl, 10 mM Hepes, pH 7.2, 1 mM $MgCl_2$, and 2 mg/ml bovine carbonic anhydrase for HCO_3^- transport, or 50 mM KCl, 50 mM Hepes, pH 7.2, and 1 mM $MgCl_2$ for Cl^- transport) containing 0.15 mM of the fluorescent pH-sensitive dye pyranine (1-hydroxypyrene-3.6.8-trisulfonic acid; Sigma-Aldrich, St. Louis, MO) for HCO_3^- transport, or 2.8 mg/ml SPQ probe for Cl^- transport (6-methoxy-N-[3-sulfopropy1]Quinolinium, Invitrogen Fisher Scientific, Illkirch, France). After 3 washes in ice-cold incubation buffer (resealing buffer without $MgCl_2$ and probe), stopped-flow experiments were performed at 30 °C for HCO_3^- transport and at 20 °C for Cl^- transport (SFM400; Bio-logic, Grenoble, France) as previously described.[12] Excitation was performed at 465nm for HCO_3^- transport (365 nm for Cl^- transport), and emitted light was filtered with a 520-nm cut-off filter for HCO_3^- transport (450 nm for Cl^- transport). For measurement of HCO_3^-/Cl^- exchange activity, dye-loaded ghosts resuspended in 3 ml *chloride buffer* (100 mM KCl and 10 mM Hepes, pH 7.2, for HCO_3^- transport, or 50 mM KCl and 50 mM Hepes, pH 7.2, for Cl^- transport) were rapidly mixed with an equal volume of bicarbonate buffer (100 mM $KHCO_3$ and 10 mM Hepes, pH 7.2, for HCO_3^- transport or 100 mM $KHCO_3^-$, 200 mM sucrose, and 10 mM Hepes, pH 7.2, for Cl^- transport), generating an inwardly directed HCO_3^-/CO_2 gradient of 50 mEq/l and an outwardly directed Cl^- gradient of equal magnitude. Data from 6 time courses were averaged and fit to a mono-exponential function using the simplex procedure of Biokine software (Bio-logic, Grenoble, France). This allowed the measurement of a transport constant (k). Then, permeability was calculated as the following equation:

$$P = k \times r/3 \quad (1)$$

where P is permeability (in $\mu m \times s^{-1}$), k is transport constant (in s^{-1}), and r is radius (in μm).

Protein Quantification

The AE1 surface expression on RBCs was detected using a FACSCanto II flow cytometer (BD BioSciences, Bedford, MA), after glutaraldehyde (0.025%) fixation and staining either with a monoclonal human anti-Diego b (1/4, HIRO 58, provided by Dr. M. Uchikawa, Japanese Red Cross Central Blood Center, Tokyo, Japan) or the mouse monoclonal Bric6 (1/40, IBGRL, Bristol, UK) antibodies. Secondary antibodies were phycoerythrin-conjugated goat anti-human and anti-mouse, respectively (1/100; Beckman Coulter, Brea, CA). Flow cytometer results were analyzed using FlowJo software (FlowJo, Ashland, OR). Eosin-5′-maleimide (EMA) dye test were also performed.[11,13] For the Coomassie blue analysis, ghosts were prepared by hypotonic lysis, providing *white* ghosts.[14] Membrane proteins from whole ghost cell lysates were separated on sodium dodecyl sulphate−polyacrylamide gel electrophoresis (4%−12% acrylamide) in reducing conditions (2.8 mM β-mercaptoethanol) and stained with Coomassie blue. The densitometric analyses of data were performed using ImageJ 1.46j software (National Institutes of Health, Bethesda, MD).

Ghost Diameter Measurements

Ghosts preparation was the same as the one for stopped flow experiments except for pyranine concentration (1.5 mM). Of the ghosts, 2% were mounted between a slide and coverslip. Ghost diameters were measured using an Axio Observer Z1 microscope with an AxioCam MRm camera (Zeiss, Marly-le-Roi, France). An average of 800 fluorescent ghosts were measured for each genotype.

Statistical Analyses

Because of the low number of values in some groups, the distribution could not be supposed as normal. Therefore, we used only nonparametric tests: the Mann−Whitney test when 2 groups were compared, and the Kruskal−Wallis test (with the Dunn multiple comparison test) when more than 2 groups were compared. Data are presented as their median and interquartile range (Q1−Q3). We considered a P value <0.05 as significant.

Data Availability

The datasets generated during and/or analyzed during the current study are available from the corresponding author on reasonable request.

RESULTS

Included Patients

Fifteen patients were included. Table 1 shows their characteristics at diagnosis. Seven were diagnosed when they were adults. In children, the earliest diagnosis was performed within the first year of life. Two patients carried the characteristic molecular anomaly associated with South Asian ovalocytosis (SAO), which corresponds to the in-frame deletion of 27 nucleotides of *SLC4A1* gene, leading to the loss of 9 amino acids (Table 2).[15−27] Those 2 patients harbored other *SLC4A1* mutations: one patient carried the recessive p.G701D mutation involved in dRTA, whereas the other carried the amino acid change p.E90K, involved in spherocytosis and the p.T581D one, involved in dRTA (Figure 1).[26] All other patients carried a missense dominant mutation. Seven were in position 589 of the protein: 4 patients had p.R589H and 3 patients had p.R589C. Three affected dRTA patients harbored

Table 1. Characteristics of included patients at diagnosis

Patient	Mutation	Sex	Age (yr)	Hb (g/l)	CrP (μM)	eGFR (ml/min per 1.73 m^2)	CO_2t (mM)	Nephrolithiasis	Nephrocalcinosis	Familial history	Dynamic test	Known RBC anomaly	Bone demineralization
1	p.R589H	M	9	NA	41	92	8	Y	N	Y	N	N	Y
2	p.R589H	F	33	11.5	94	61	20	Y	Y	Y	N	N	N
3	p.R589H	M	45	14.9	115	57	21	Y	Y	Y	Y	N	N
4	p.R589C	F	25	13.2	73	89	22	Y	Y	Y	Y	Iron deficiency	N
5	p.R589H	F	2	13.0	71	>90	21	Y	Y	Y	N	N	Y
6	p.E906*	M	30	17.5	142	52	23	Y	Y	Y	Y	Polycythemia	N
7	p.S613F	F	20	12.5	76	74	23	Y	Y	Y	N	N	N
8	p.R589C	F	2	11.1	36	103	13	N	Y	N	N	Elliptocytes	Y
9	p.R589C	F	1	NA	NA	NA	NA	Y	Y	N	Y	N	NA
10	p.D905dup	M	9	NA	75	71	NA	Y	Y	N	Y	N	NA
11	p.E906K	M	44	13.1	80	103	23	Y	N	Y	Y	N	N
12	p.G609R	M	34	9.4	196	36	8	Y	Y	Y	N	N	NA
13	p.S525F	F	14	NA	62	125	14	Y	Y	N	Y	N	N
14	del27/p.G701D	F	2	13.0	88	74	19	Y	Y	N	Y	Anisocytes, macrocytes, stomatocytes	N
15	p.E90K/p.T581D/ del27	M	9	13.0	40	77	15	N	Y	N	N	Ovalocytes	Y

CrP, creatininemia; eGFR, estimated glomerular filtration rate; F, female; Hb, hemoglobin; M, male; N, no; NA, information not available; Y, yes.
Distal renal tubular acidosis was assessed by a dynamic test ($\Delta U\text{-}B_{PCO2}$), acute acid load, and/or the furosemide–fludrocortisone test) in 8 patients. All patients experienced nephrolithiasis and/or nephrocalcinosis. Five patients had known red blood cell (RBC) morphological anomalies.

missense p.S613F, p.E906*, and p.G609R mutations, whereas 1 patient carried a duplication (p.D905dup). Interestingly, 2 patients exhibited nonreported mutations (p.E906K and p.S525F). According to the guidelines of the American College of Medical Genetics and Genomics,[27] we found 16 of them to be pathogenic or likely pathogenic (class 5 and 4, respectively), whereas 2 more were of uncertain significance (i.e., class 3).

Three patients had chronic kidney disease as defined by an estimated glomerular filtration rate of <60 ml/min per 1.73 m^2, and 6 patients had overt metabolic acidosis as defined by $[HCO_3^-]$ <20 mM. All patients had a history of nephrolithiasis and/or nephrocalcinosis. Six patients did not have a familial history of renal/metabolic injury. Dynamic testing of renal acidification was performed in 8 patients: 2 had an abnormal $\Delta U\text{-}B(PCO_2)$,[28]

Table 2. Mutations in the *SLC4A1* gene expressed by included patients

Patient	Sex	Age (yr)	Short-name mutation	Nucleotide	Protein	Type of mutation	Localization	Reference	Exon	*In vitro* data reference	Class ACMG 2015
1	M	13	p.R589C	c.1765C>T	p.Arg589Cys	5	TM6	15	14	315, 16	PS3, PS4, PM1, PM2, PP3, PP5
2	F	41	p.R589H	c.1766G>A	p.Arg589His	5	TM6	15	14	15–17	PS3, PS4, PM1, PM2, PP3, PP5
3	M	70	p.R589H	c.1766G>A	p.Arg589His	5	TM6	15	14	15–17	PS3, PS4, PM1, PM2, PP3, PP5
4	F	30	p.R589C	c.1765C>T	p.Arg589Cys	5	TM6	15	14	15, 16	PS3, PS4, PM1, PM2, PP3, PP5
5	F	22	p.R589H	c.1766G>A	p.Arg589His	5	TM6	15	14	15–17	PS3, PS4, PM1, PM2, PP3, PP5
6	M	34	p.E906*	c.2716G>T	p.Glu906*	5	C-ter	18	20	Not described	PVS1, PM1, PM2
7	F	55	p.S613F	c.1838C>T	p.Ser613Phe	5	TM7	15	15	315, 17	PS3, PM1, PM2, PP3, PP5
8	F	15	p.R589C	c.1765C>T	p.Arg589Cys	5	TM6	15	14	15,16	PS3, PS4, PM1, PM2, PP3, PP5
9	F	28	p.R589C	c.1765C>T	p.Arg589Cys	5	TM6	15	14	15, 16	PS3, PS4, PM1, PM2, PP3, PP5
10	M	52	p.D905dup	c.2715_2717dup	p.Asp905dup	4	C-ter	19	20	Not described	PM1, PM2, PM4, PP5
11	M	47	p.E906K	c.2716G>A	p.Glu906Lys	4	C-ter	Not described	20	Not described	PM1, PM2, PM5
12	M	29	p.G609R	c.1825G>A	p.Gly609Arg	5	TM7	20	15	20	PS3, PM1, PM2, PP3, PP5
13	F	28	p.S525F	c.1574C>T	p.Ser525Phe	3	TM5	Not described	13	Not described	PM1, PM2, PP3
Ovalocytosis											
14	F	25	p.G701D	c.2102G>A	p.Gly701Asp	5	ICL8-9	21	17	17, 21, 22	PS3, PM1, PM2, PP3, PP5
			del27	c.1199_1225del	p.Ala400_Ala408del	4	TM1	23	11	Not described	PM2, PM4, PP3, PP5
15	M	11	p.E90K	c.268G>A	p.Glu90Lys	4	N-ter	24	5	Not described	PS3, PM1, PM2, PP5
			p.T581D	c.1742C>A	p.Thr581Asn	3	TM6	25	14	Not described	PM1, PM2
			del27	c.1199_1225del	p.Ala400_Ala408del	4	TM1	23	11	Not described	PM2, PM4, PP3, PP5

F, female; M, male.
A total of 18 (12 different) gene mutations were identified in 15 patients. Two were predicted *in silico,* whereas 10 were previously reported. Thirteen patients had dominant distal renal tubular acidosis (dRTA). Three mutations were located at the C-terminal (C-term) domain, whereas 1 was found at the N-terminal (N-term) domain and 1 in the intracellular loop (ICL) between transmembrane domain (TM) 8 and TM9. Eight, 2, and 2 were found in TM6, TM7, and TM1, respectively. Following the American College of Medical Genetics (ACMG) recommendations published previously,[26] variants were classified into 5 categories (class 1, benign; class 2, likely benign; class 3, uncertain significance; class 4, likely pathogenic; and class 5, pathogenic) based on several criteria including population data, computational data, functional data, and segregation data. These criteria are weighted as very strong (PVS1), strong (PS1–4); moderate (PM1–6), or supporting (PP1–5). The mutations previously reported are presented with their references, as well as the references for the *in vitro* characterization of the mutation showing their pathogenicity.

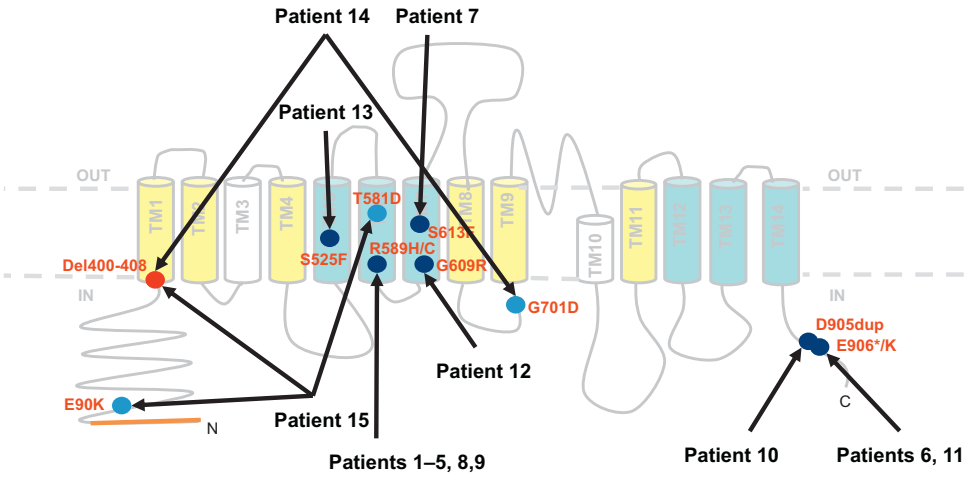

Figure 1. Localizations of mutations carried by included patients. This 2-dimensional representation of anion exchanger 1 (AE1) protein inserted into the cell membrane shows the precise localization of the 12 different mutations identified in our cohort of patients (Pt). Red dot shows the typical deletion of 27 base pairs (i.e., 9 aminoacids) found in South Asian ovalocytosis (SAO). Blue dots show the mutations involved in distal renal tubular acidosis (dRTA): light and dark dots indicate recessive and dominant mutations, respectively. The 65 missing aminoacids at the N-terminal part of the kidney isoform of AE1 (kAE1) are represented in orange. The 14 transmembrane domains (TM) belonging to the core and the gate are colored in yellow and cyan, respectively.[26]

2 others had an abnormal response to the acute acid load test,[29] and 4 more had an abnormal response to the furosemide–fludrocortisone test[30] (among those patients, 3 had also an abnormal response to the acute acid load test). Bone demineralization was reported in 4 patients.

Routine Hematological Analysis

No patient exhibited either overt anemia or other hemoglobinopathy (such as thalassemia or sickle cell disease). All had a normal mean corpuscular volume, and none had any anomalies in blood cells counts (Table 3) at the time of inclusion. No cytological

Table 3. Biology at inclusion

Patient	Short-name mutation	Age (yr)	Sex	WBCs (10^9/l)	RBCs (10^{12}/l)	Hb (g/dl)	MCV (fl)	Platelets (10^9/l)	MCH (pg/cell)	MCH (g/l)	Reticulocytes (10^9/l)	Elmax[a]	Omin[b] (Osm/kgH_2O)	Ohyper[c] (Osm/kgH_2O)
1	p.R589H	13	M	6.72	4.80	13.9	84.4	274	29.0	34.3	42.7	0.55	142	404
2	p.R589H	41	F	10.62	5.25	14.5	93.0	257	27.6	29.7	81.9	0.56	161	457
3	p.R589H	70	M	6.17	5.32	16.0	99.1	254	30.1	30.4	64.9	0.56	155	447
4	p.R589C	30	F	5.58	4.41	13.6	99.8	204	30.8	30.9	50.7	0.58	160	443
5	p.R589H	22	F	11.38	4.81	13.9	95.0	252	28.9	30.4	46.7	0.56	154	446
6	p.E906*	34	M	8.11	5.91	17.3	97.0	271	29.3	30.2	66.8	0.55	171	452
7	p.S613F	55	F	6.28	3.8	12.0	106.3	170	31.6	29.7	35.3	0.57	164	457
8	p.R589C	15	F	9.10	4.74	11.9	77.0	407	25.1	32.6	30.3	0.52	120	385
9	p.R589C	28	F	6.98	3.96	12.1	87.9	189	34.8	30.6	84.4	0.55	150	414
10	p.D905dup	52	M	5.29	5.03	15.0	90.3	176	29.8	33.0	61.9	0.55	156	420
11	p.E906K	47	M	5.66	4.47	12.9	94.2	272	28.9	30.6	80.9	0.58	154	452
12	p.G609R	29	M	7.81	4.13	11.5	87.9	180	27.8	31.7	73.9	0.57	144	452
13	p.S525F	28	F	4.57	4.59	13.3	87.1	240	29.0	33.3	47.7	0.58	155	456
Ovalocytosis														
14	del27/ p.G701D	25	F	10.86	3.58	14.4	111.7	488	40.2	36.0	190.8	0.29	79	240
15	del27/p.E90K/ p.T581D	11	M	9.32	5.62	12.8	73.2	499	22.7	31.0	120.6	0.00	NA	NA
	Median	29		6.98	4.74	13.6	93.0	254	29.0	30.9	64.9	0.56	155	447
	Q1	24		5.92	4.27	12.5	87.5	197	28.4	30.4	47.2	0.55	146	420
	Q3	44		9.21	5.14	14.5	98.1	273	30.5	32.8	81.4	0.57	159	452

F, female; Hb, hemoglobin; M, male; MCH, mean corpuscular hemoglobin; MCV, mean corpuscular volume in femtoliter (fl); NA, not applicable; Q1, first quartile; Q3, third quartile; RBCs, red blood cells; WBCs, white blood cells.
[a]Elmax: corresponds to the maximal deformability index or elongation index (EI).
[b]Omin: reflects the surface area/volume ratio and corresponds to the osmolality at the minimal deformability in hypo-osmolar area, or at the osmolality when 50% of the red cells hemolyzed during the regular osmotic resistance test.
[c]Ohyper: corresponds to the osmolality at half of the DImax and reflects the hydration state of the RBCs.
No patient exhibited severe anemia at the time of inclusion.

anomaly was detected in RBCs from dRTA patients without SAO (dRTA SAO−), although we observed the characteristic defects in RBCs from SAO patients (dRTA SAO+): ovalocytes and very large RBCs, exhibiting 1 or 2 curvilinear transverse strips (Figure 2). The RBC deformability (EImax), surface area-to-volume ratio (Omin), and hydration state (Ohyper) of RBCs from dRTA SAO− patients did not significantly differ as compared to those of controls. As expected, only dRTA SAO+ patients had a large decreased RBC deformability (EImax) with almost nonmeasurable ektacytometry parameters (Table 3, Figure 2 lower panel). dRTA SAO− patients did not exert either clinical or biological overt anomalies; moreover, their RBC membranes seemed to be comparable to those of the controls subjects. Only dRTA SAO+ exerted severe morphological RBC membrane dysfunction.

Bicarbonate and Chloride Transports Through Red Blood Cell Membranes

Figure 3 shows the transport of HCO_3^- and Cl^- in ghosts. Diameters of ghosts (Figure 3a) obtained after RBC hypotonic lysis and resealing were not significantly different between groups (median 6.25, 5.88, and 7.67 μm in controls, dRTA SAO−, and dRTA SAO+, respectively), and hence surfaces of exchange were not significantly different (123, 108, and 185 μm^2 in controls, dRTA SAO−, and dRTA SAO+, respectively). Transport constants (k) for HCO_3^- (Figure 3b) and Cl^- (Figure 3c) were significantly lower in dRTA SAO+ as compared to those in dRTA SAO−. Even though all dRTA SAO− patients had measurements close to those of the controls, the patient with the p.S525F mutation had k(HCO_3^-) values very close to those measured in dRTA SAO+. Taken together, the relative values of k(HCO_3^-) and k(Cl^-) allowed us to distinguish clearly dRTA SAO+, whereas dRTA SAO− were merged within the controls (as plotted in Figure 3d). For the patients in whom we measured surface of exchange, the calculated relative permeabilities (P) were lower in dRTA SAO+ than in the dRTA SAO− patients for both HCO_3^- and Cl^-, confirming the distinction between dRTA SAO+ to the others (Figure 3e). Thus, dRTA SAO− express an AE1 protein that is capable of normal anion transports, whereas only dRTA SAO+ exhibit severe impairment in AE1-dependent anion exchange.

AE1 Expression in Red Blood Cells

To determine whether the lower transport activity of AE1 in dRTA SAO+ patients is related to lower membrane AE1 expression or to an intrinsic transport defect, we quantified its membrane expression (Figure 4). We used 3 different probes: EMA, Bric6, and Diego b (Figure 4b) that all recognize extracellular parts of the protein. Flow cytometry analysis

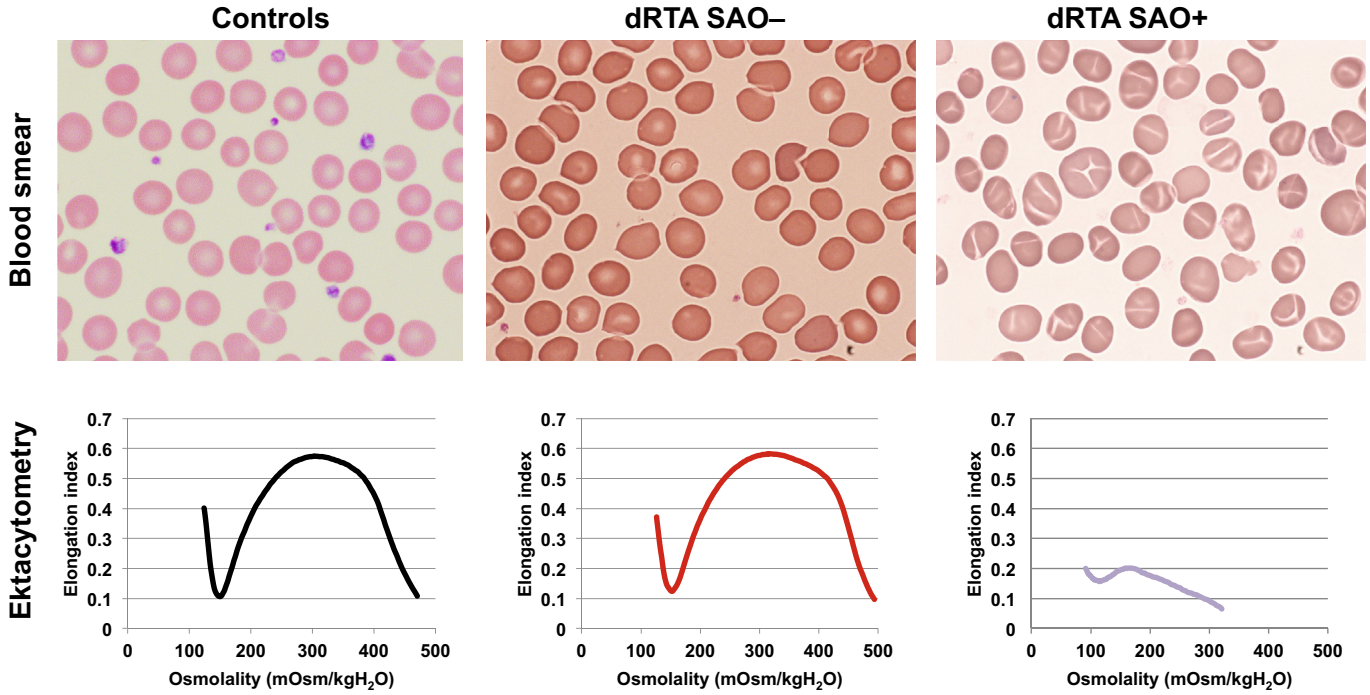

Figure 2. Red blood cells from included patients. (Upper panels) Blood smears after May−Grünwald Giemsa coloration (MGG) in healthy controls, in patients exerting a dominant mutation in the *SLC4A1* gene leading to distal renal tubular acidosis (dRTA SAO−), and patients exerting a mutation in the *SLC4A1* gene leading to South Asian Ovalocytosis (SAO) in addition to the one leading to dRTA (dRTA SAO+). (Lower panels) Ektacytometry curves revealed a dramatic decrease in the elongation indexes only in the dRTA SAO+ affected patients, where they were normal in the dRTA SAO− patients.

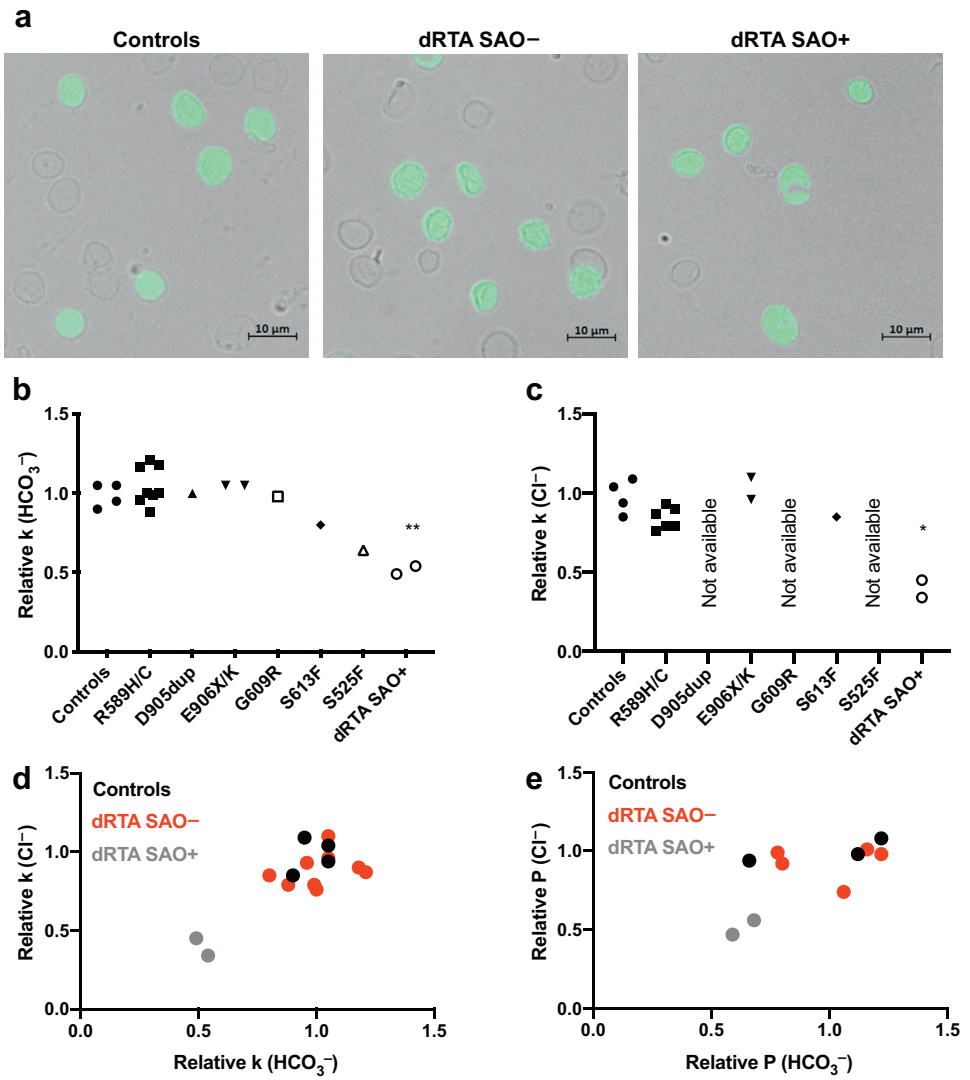

Figure 3. Transports of HCO_3^- and Cl^- in ghosts from patients with mutations in AE1 gene and controls. (a) From circulating red blood cells (RBCs), ghosts were resealed with pyranine to measure volume and membrane surface. (b,c) Relative values of transport (k) of both (b) HCO_3^- and (c) Cl^- were significantly decreased in patients exerting a mutation in the *SLC4A1* gene leading to South Asian ovalocytosis (SAO) in addition to that leading to dRTA (dRTA SAO+), as compared to the other patients exerting a mutation in the *SLC4A1* gene leading to a dRTA but without SAO (dRTA SAO−), as well as controls. (d,e) HCO_3^- and Cl^- k and permeability (P) were correlated with each other and were strongly different in dRTA SAO+ as compared to the other.

(Figure 4a) showed a reduced labeling in dRTA SAO+ patients (52%) compared with that in controls (100%) ($P < 0.05$) or dRTA SAO− (104%) as labeled with EMA, Bric6 (14%), or Diego b (54%). It is noteworthy that the patient with p.S525F mutation exhibited similar values to those of dRTA SAO− and controls. We also quantified the total amount of protein present in RBC membranes by quantifying the third band (i.e., band 3) by Coomassie blue staining after gel electrophoresis (Figure 4c). No difference was observed between controls, dRTA SAO−, and dRTA SAO+ for the density of band 3 ($P = 0.26$) even when band 3 density was normalized to the density of all polypeptides from same lane ($P = 0.37$) (Figure 4d).

Taken together, the aforementioned results indicate that expression of band 3 in dRTA SAO− is normal. In dRTA SAO+, AE1 membrane expression is decreased, whereas the total amount of AE1 protein remains normal.

Finally, we show that only patients with SAO mutation exert severe RBC morphological anomalies with a large decrease in band 3 transport function that seems to be related to its membrane expression, whereas in dRTA patients without SAO mutation, both functional (transport) and morphological functions are preserved.

DISCUSSION

Taken together, our data show that mutations in *SLC4A1* gene associated with dominant dRTA do not affect the function of the erythroid isoform band 3 unless the patient has an additional deletion causing

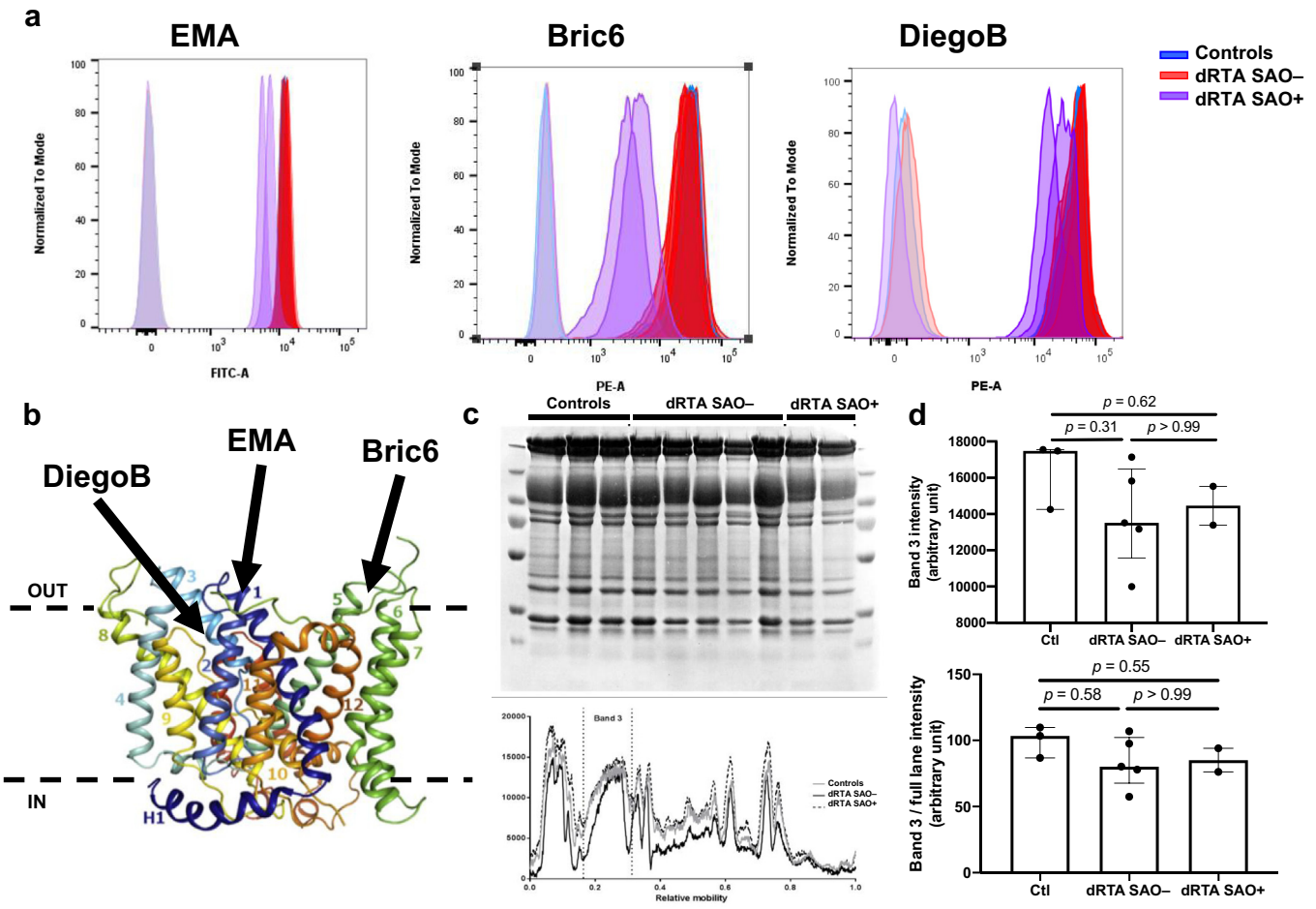

Figure 4. AE1 protein expression at red blood cell (RBC) membrane. (a) Membrane expression of AE1 was studied in ghosts from RBCs by flow cytometry with 3 different probes: EMA, Bric6, and Diego B. (b) These 3 probes recognize 3 different extracellular domains of the AE protein. (c) Coomassie staining is shown with its intensity. (d) Quantifications of the intensity of band 3 (top) and band 3/full lane (bottom) did not show any difference.

SAO. The stopped-flow spectrophotometry analyses that we report in this context have some limitations. First, to measure the HCO_3^- transport, we used an intracellular pH-sensitive probe (pyranine) as a proxy (not the direct HCO_3^- concentration): we also report here results with the SPQ probe (measuring Cl^- concentration), the results of which are highly correlated with those of pyranine ($r^2 = 0.62$, $P < 0.0001$). Previous reports have also shown similar results in heterologous models (*Xenopus* oocytes).[31,32] or by using sulfate as a surrogate for chloride transport.[32] Second, the intracellular pH also depends on the carbonic anhydrase activity: to blunt this limiting step, we saturated the intracellular compartment with 2 mg/ml bovine carbonic anhydrase in every ghost. Finally, the systemic acidosis could impair the function of the AE1 protein: of note, patients with the most (acidotic) phenotype (at least at diagnosis) were not the ones carrying a SAO mutation.

Nonetheless, this is the first report of in-depth assessment of RBC membrane disorders in patients with AE1-related dRTA. Very recently, an international cohort of dRTA patients was reported with many data on both the phenotypic diagnosis and evolution,[18] but the authors did not collect any hematological data. Previous studies that focused on the correlation between hematological and renal involvements of AE1 mutations were performed in patients carrying recessive mutations (mostly p.G701D) and the specific SAO deletion.[33–35] Moreover, when RBC anomalies were investigated, the authors reported only RBC shape and hemoglobin concentrations. Here, we report data on the transport activity of band 3 in RBCs and on the membrane/cytoskeleton relationship, as well as of RBC shape and hemoglobin concentration. Other reports have also shown that *SLC4A1* gene mutations are the main observed anomalies in dRTA, not only in Europe,[18] but also in south Asia.[36] Obvious hematological anomalies appear to be present only if patients carry the specific SAO anomaly,[23] which is consistent with our findings.

Knowing the precise (RBC) phenotype of patients bearing AE1 mutations could be of high interest at the time of the molecular diagnosis: as stated in the guidelines on the interpretation of molecular data,[27] the exponential development of molecular diagnoses leads

to the discovery of new *variants*, for which interpretation could be very challenging. As an example, the patient carrying the p.S525F mutation had a class 3 variant (i.e., *of uncertain significance*). Interestingly, she had the lowest $k(HCO_3^-)$ and $P(HCO_3^-)$ values within the dRTA SAO− patients. Unfortunately, we did not have enough material to measure $k(Cl^-)/P(Cl^-)$. Moreover, the transport of both Cl^- and HCO_3^- in patients carrying a mutation in position 589 appeared to be indistinguishable from those of controls. Most of the other mutations seem to have a behavior similar to that of p.R589H/C. Results from p.S525F remain questionable: RBC phenotype (transport) could lead to the interpretation of it as a differential genotype/phenotype correlation and could argue for a functional implication in the phenotype/disease (dRTA), bringing this *variant* to pathogenic, as it occurs in the domain important for the dimerization of the protein.

The recent crystallization structure of band 3[26] and structural analyses[4] help in understanding the differential mechanisms involved in several structural RBC diseases and the wide spectrum of interactions that AE1 develops with other proteins. In RBCs, the full-length AE1 is expressed as oligomers (di- and tetramers)[1]: the dimers interact with cytosolic enzymes (such as aldolase, glyceraldehye-3-phosphate dehydrogenase, and carbonic anhydrase) at both the C- and N-terminal parts of the protein, whereas the tetramers interact with protein 4.2 and ankyrin, anchoring the complex (and thus the membrane) to the cytoskeleton. The interaction between AE1 and ankyrin (and thus the cytoskeleton) has also been shown in renal cells.[9] This is of particular importance, as some mutations in the *SLC4A1* locus lead to a defect in this specific interaction with the cytoskeleton, and then lead to an impaired RBC shape called *hereditary spherocytosis*.[37]

The fact that transport function of kAE1 leading to dRTA is impaired, whereas that of band 3 is preserved, argues for a rescue capacity in RBC. Besides the cytosolic interactions, RBC AE1 also interacts with membrane protein, such as glycophorin A (GPA). As with cytosolic proteins (such as ankyrin and stomatin[14]), the interaction with GPA can modify or alter the conformation and the function of AE1.[38] More precisely, GPA could act as a protective chaperone by maintaining AE1 membrane expression.[39] That is consistent with the fact that in dRTA, kAE1 is less expressed at the membrane and is retained within the Golgi apparatus of kidney cells.[40] This could be related to other chaperones that avoid its expression (and function) at the α-ICs membrane. Further studies are needed to test whether modifying kAE1 expression by modulating chaperone function(s) could restore renal acidification ability.

Here, we also report differences in the quantitative assessment of band 3 expression in RBC from SAO patients: when assessed by labeling of extracellular domains of the protein, RBC membranes from SAO patients exhibited a decreased expression of AE1, whereas when assessed by total protein abundance, AE1 expression was not impaired, as previously reported.[31,32] This could be related to such an important modification in the conformation of the protein that epitopes detected by immunolabeling could not be recognized, but the mobility shift previously reported[31] was not detected here.

In conclusion, AE1 dominant mutants associated with dRTA (i.e., known to alter transport in kidney) exert normal transport in RBCs. Transport in RBCs is altered only when the SAO mutant is additionally present.

DISCLOSURE

All the authors declared no competing interests.

ACKNOWLEDGMENTS

J-PB, SG, LDC, and IM-C received funding from the laboratory of excellence for Red cells (LABEX GR-Ex)-ANR Avenir-11-LABX-0005-02. DE is funded by grant from l'Agence Nationale de la Recherche (ANR BLANC 14-CE12-0013-01/HYPERSCREEN) and from Philancia. The authors are grateful to the patients (and their families) affected with dRTA and/or South Asian ovalocytosis who participated to this study. The authors also thank O. Fenneteau for the red blood cell images and H. Bourdeau for technical assistance on eosin-5′-maleimide and ektacytometry.

REFERENCES

1. Cordat E, Reithmeier RA. Structure, function, and trafficking of SLC4 and SLC26 anion transporters. *Curr Top Membr*. 2014;73:1–67.
2. Reithmeier RA, Casey JR, Kalli AC, et al. Band 3, the human red cell chloride/bicarbonate anion exchanger (AE1, SLC4A1), in a structural context. *Biochim Biophys Acta*. 2016;1858:1507–1532.
3. Perrotta S, Gallagher PG, Mohandas N. Hereditary spherocytosis. *Lancet*. 2008;372:1411–1426.
4. Rivera-Santiago R, Harper SL, Sriswasdi S, et al. Full-length anion exchanger 1 structure and interactions with ankyrin-1 determined by zero length crosslinking of erythrocyte membranes. *Structure*. 2017;25:132–145.
5. Da Costa L, Galimand J, Fenneteau O, et al. Hereditary spherocytosis, elliptocytosis, and other red cell membrane disorders. *Blood Rev*. 2013;27:167–178.
6. Eladari D, Kumai Y. Renal acid-base regulation: new insights from animal models. *Pflugers Arch*. 2015;467:1623–1641.
7. Alexander RT, Cordat E, Chambrey R, et al. Acidosis and urinary calcium excretion: insights from genetic disorders. *J Am Soc Nephrol*. 2016;27:3511–3520.

8. Palazzo V, Provenzano A, Becherucci F, et al. The genetic and clinical spectrum of a large cohort of patients with distal renal tubular acidosis. *Kidney Int*. 2017;91:1243–1255.
9. Genetet S, Ripoche P, Le Van Kim C, et al. Evidence of a structural and functional ammonium transporter RhBG.anion exchanger 1.ankyrin-G complex in kidney epithelial cells. *J Biol Chem*. 2015;290:6925–6936.
10. Mumtaz R, Trepiccione F, Hennings JC, et al. Intercalated cell depletion and vacuolar H(+)-ATPase mistargeting in an Ae1 R607H knockin model. *J Am Soc Nephrol*. 2017;28:1507–1520.
11. Da Costa L, Suner L, Galimand J, et al. Diagnostic tool for red blood cell membrane disorders: assessment of a new generation ektacytometer. *Blood Cells Mol Dis*. 2016;56:9–22.
12. Frumence E, Genetet S, Ripoche P, et al. Rapid Cl(-)/HCO(-)(3) exchange kinetics of AE1 in HEK293 cells and hereditary stomatocytosis red blood cells. *Am J Physiol Cell Physiol*. 2013;305:C654–C662.
13. King MJ, Behrens J, Rogers C, et al. Rapid flow cytometric test for the diagnosis of membrane cytoskeleton-associated haemolytic anaemia. *Br J Haematol*. 2000;111:924–933.
14. Genetet S, Desrames A, Chouali Y, et al. Stomatin modulates the activity of the anion exchanger 1 (AE1, SLC4A1). *Sci Rep*. 2017;7:46170.
15. Bruce LJ, Cope DL, Jones GK, et al. Familial distal renal tubular acidosis is associated with mutations in the red cell anion exchanger (Band 3, AE1) gene. *J Clin Invest*. 1997;100:1693–1707.
16. Quilty JA, Li J, Reithmeier RA. Impaired trafficking of distal renal tubular acidosis mutants of the human kidney anion exchanger kAE1. *Am J Physiol Renal Physiol*. 2002;282:F810–F820.
17. Cordat E, Kittanakom S, Yenchitsomanus PT, et al. Dominant and recessive distal renal tubular acidosis mutations of kidney anion exchanger 1 induce distinct trafficking defects in MDCK cells. *Traffic*. 2006;7:117–128.
18. Lopez-Garcia SC, Emma F, Walsh SB, et al. Treatment and long-term outcome in primary distal renal tubular acidosis. *Nephrol Dial Transplant*. 2019;34:981–991.
19. Zhang Z, Liu KX, He JW, et al. Identification of two novel mutations in the SLC4A1 gene in two unrelated Chinese families with distal renal tubular acidosis. *Arch Med Res*. 2012;43:298–304.
20. Rungroj N, Devonald MA, Cuthbert AW, et al. A novel missense mutation in AE1 causing autosomal dominant distal renal tubular acidosis retains normal transport function but is mistargeted in polarized epithelial cells. *J Biol Chem*. 2004;279:13833–13838.
21. Tanphaichitr VS, Sumboonnanonda A, Ideguchi H, et al. Novel AE1 mutations in recessive distal renal tubular acidosis. Loss-of-function is rescued by glycophorin A. *J Clin Invest*. 1998;102:2173–2179.
22. Kittanakom S, Cordat E, Akkarapatumwong V, et al. Trafficking defects of a novel autosomal recessive distal renal tubular acidosis mutant (S773P) of the human kidney anion exchanger (kAE1). *J Biol Chem*. 2004;279:40960–40971.
23. Besouw MTP, Bienias M, Walsh P, et al. Clinical and molecular aspects of distal renal tubular acidosis in children. *Pediatr Nephrol*. 2017;32:987–996.
24. Bracher NA, Lyons CA, Wessels G, et al. Band 3 Cape Town (E90K) causes severe hereditary spherocytosis in combination with Band 3 Prague III. *Br J Haematol*. 2001;113:689–693.
25. Ashton EJ, Legrand A, Benoit V, et al. Simultaneous sequencing of 37 genes identified causative mutations in the majority of children with renal tubulopathies. *Kidney Int*. 2018;93:961–967.
26. Arakawa T, Kobayashi-Yurugi T, Alguel Y, et al. Crystal structure of the anion exchanger domain of human erythrocyte Band 3. *Science*. 2015;350:680–684.
27. Richards S, Aziz N, Bale S, et al. Standards and guidelines for the interpretation of sequence variants: a joint consensus recommendation of the American College of Medical Genetics and Genomics and the Association for Molecular Pathology. *Genet Med*. 2015;17:405–424.
28. DuBose TD Jr, Caflisch CR. Validation of the difference in urine and blood carbon dioxide tension during bicarbonate loading as an index of distal nephron acidification in experimental models of distal renal tubular acidosis. *J Clin Invest*. 1985;75:1116–1123.
29. Wrong O, Davies HE. The excretion of acid in renal disease. *Q J Med*. 1959;28:259–313.
30. Walsh SB, Shirley DG, Wrong OM, et al. Urinary acidification assessed by simultaneous furosemide and fludrocortisone treatment: an alternative to ammonium chloride. *Kidney Int*. 2007;71:1310–1316.
31. Bruce LJ, Wrong O, Toye AM, et al. Band 3 mutations, renal tubular acidosis and South-East Asian ovalocytosis in Malaysia and Papua New Guinea: loss of up to 95% Band 3 transport in red cells. *Biochem J*. 2000;350:41–51.
32. Schofield AE, Reardon DM, Tanner MJ. Defective anion transport activity of the abnormal band 3 in hereditary ovalocytic red blood cells. *Nature*. 1992;355:836–838.
33. Khositseth S, Sirikanaerat A, Khoprasert S, et al. Hematological abnormalities in patients with distal renal tubular acidosis and hemoglobinopathies. *Am J Hematol*. 2008;83:465–471.
34. Khositseth S, Sirikanerat A, Wongbenjarat K, et al. Distal renal tubular acidosis associated with anion exchanger 1 mutations in children in Thailand. *Am J Kidney Dis*. 2007;49:841–850.
35. Khositseth S, Bruce LJ, Walsh SB, et al. Tropical distal renal tubular acidosis: clinical and epidemiological studies in 78 patients. *Q J Med*. 2012;105:861–877.
36. Park E, Cho MH, Hyun HS, et al. Genotype-phenotype analysis in pediatric patients with distal renal tubular acidosis. *Kidney Blood Press Res*. 2018;43:513–521.
37. Low PS, Zhang D, Bolin JT. Localization of mutations leading to altered cell shape and anion transport in the crystal structure of the cytoplasmic domain of Band 3. *Blood Cells Mol Dis*. 2001;27:81–84.
38. Kalli AC, Reithmeier RAF. Interaction of the human erythrocyte Band 3 anion exchanger 1 (AE1, SLC4A1) with lipids and glycophorin A: molecular organization of the Wright (Wr) blood group antigen. *PLoS Comput Biol*. 2018;14:e1006284.
39. Williamson RC, Toye AM. Glycophorin A: Band 3 aid. *Blood Cells Mol Dis*. 2008;41:35–43.
40. Patterson ST, Reithmeier RA. Cell surface rescue of kidney anion exchanger 1 mutants by disruption of chaperone interactions. *J Biol Chem*. 2010;285:33423–33434.